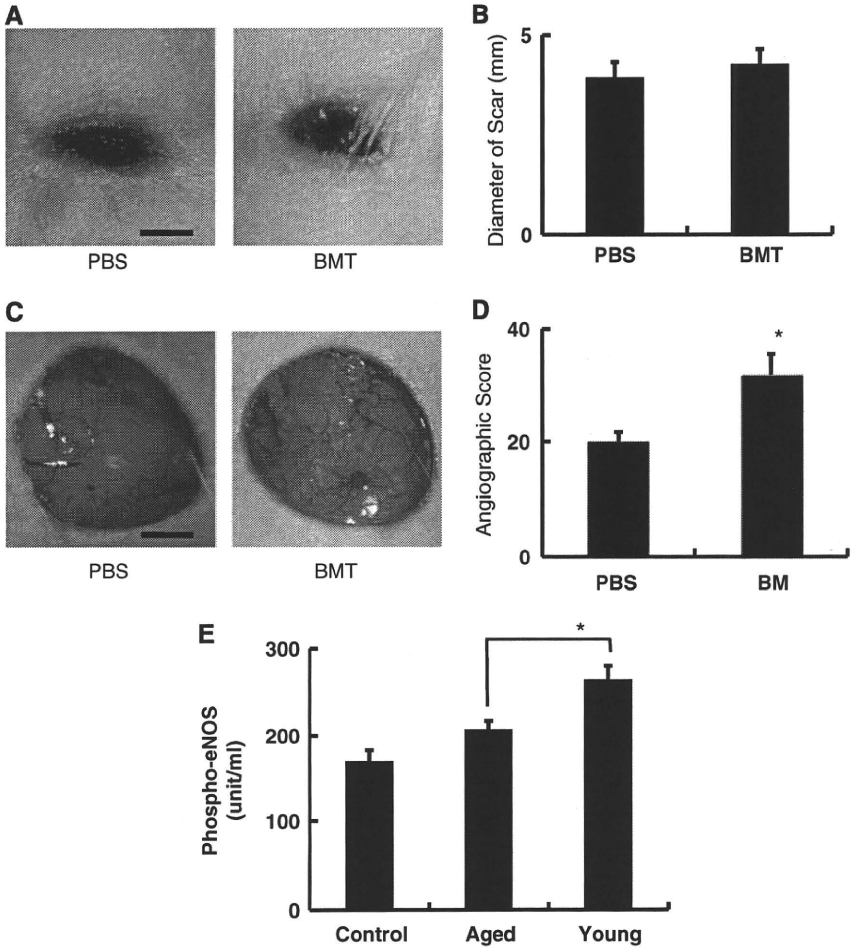

Figure 4 Endothelial cell activation: effect of bone marrow cells *in vivo* and *in vitro*. (**A**) Representative picture on day 10 after skin injury induced in aged rats treated with phosphate-buffered saline (PBS) or subject to bone marrow transplanted (BMT) with bone marrow from young rats (as described in the text). (**B**) There was no significant difference in the size of the residual wound on day 10 after skin injury comparing the two groups. (**C**, **D**) Representative photograph 30 seconds after skin injury. (**C**) A significant increase in the number of activated microvascular structures under the skin was observed in aged animals in the BMT group (the procedure for quantification of the angiographic score is described in the Materials and methods section) (**D**). (**E**) *In vitro* analysis revealed the enhanced activation of endothelial nitric oxide synthase (eNOS) in cultured human umbilical vein endothelial cells (HUVECs) exposed to bone marrow mononuclear cells harvested from young animals, versus those harvested from aged animals. $*P < 0.05$ versus PBS control (**D**) or aged bone marrow (**E**). $n = 5$, in each group. Scale bar: 2 mm.

monitored repair of full-thickness skin wounds made on the backs of animals using a biopsy punch. On day 10 after injury, the size of the scar was measured. No significant difference in the size of wounds was observed between animals transplanted with young bone marrow cells or PBS controls (Figures 4A and 4B). However, low power micrographs soon after injury (30 seconds) displayed many more visually apparent vascular structures in wounds from animals receiving transplanted cells from young animals compared with PBS controls (Figures 4C and 4D). As the latter occurred quickly after injury, it could be considered an acute vascular response to the skin wound (i.e., activation of microvasculature involving recruitment of additional channels or dilation of channels already subject to blood flow) rather than formation of new vascular channels, which would, presumably, require additional time.

The above observation suggested the possibility that activation of endothelial cells might occur more readily in the presence of bone marrow cells. To assess this possibility *in vitro*, HUVECs were cultured in the presence of bone marrow mononuclear cells derived from young (4 weeks old) or aged (50 weeks old) SHR-SP. As an index of endothelial activation, phosphorylation of eNOS in HUVECs was monitored. Endothelial cells cocultured with bone marrow-derived mononuclear cells from young animals displayed a higher level of phospho-eNOS, compared with HUVECs exposed to bone marrow cells from aged rats (Figure 4E).

Transplantation of Bone Marrow from Young Animals Impacts on the Cerebral Microvasculature Poststroke

To investigate the possible mechanisms underlying reduced brain damage observed poststroke in aged rats subject to transplantation with bone marrow cells from young animals, cerebrovascular density and proliferation were studied 30 days after induction of stroke. Compared with PBS-injected rats (Figure 5A), vascular density in the peristroke area of transplanted animals showed a significant increase in vascular density (Figures 5B and 5C). In contrast, there was no significant difference in the density of vasculature in the contralateral cortex comparing animals treated with PBS (Figure 5D) or bone marrow transplantation (Figures 5E and 5F). To evaluate the effect of aging on vascular density, cerebral infarction was induced in 8-week-old SHR-SP, and the density of vasculature was evaluated. The results demonstrate a significantly higher vascular density in the peristroke area (Figures 5G and 5H) and contralateral cortex (Figures 5I and 5J) in young rats compared with aged rats. These results are consistent with previous reports that cerebrovascular density decreases with aging (Hutchins *et al*, 1996; Lynch *et al*, 1999; Sonntag *et al*, 1997). To investigate proliferation of endothelium in the cerebrovasculature of the cerebral cortex, cells coexpressing Ki67 and Lectin were investigated. However, the number of cells expressing both markers was too small (mean number of double-positive cells was less than one cell per section in both group) to perform quantitative analysis and obtain meaningful data.

To evaluate the effects of bone marrow cells on endothelial cells, activation of MAP kinases was evaluated *in vitro*. The MAP kinases are serine/threonine-specific protein kinases that regulate critical cellular activities, such as mitosis, differentiation, and cell survival/apoptosis (Kant *et al*, 2006). Exposure of cultured endothelial cells to bone marrow mononuclear cells from young animals resulted in decreased levels of phospo-p38 compared with endothelial cells exposed to bone marrow from older rats (Figure 5K). As the latter is consistent with decreased activation of p38 (activation of p38 in endothelium induces apoptotic death through a mitochondrial pathway) (Mehta *et al*, 2007), it would suggest a basis for increased survival of endothelial cells in the presence of bone marrow mononuclear cells from young animals. In contrast, there were no significant differences in the phosphorylation of two other MAP kinases, ERK1/2 and JNK1/2, comparing the two groups (data not shown). These results are consistent with our *in vivo* observation that transplantation of young bone marrow into aged mice has little impact on endothelial proliferation, but enhances the density of microvasculature in the peristroke area.

To investigate the effect of transplantation of bone marrow from young mice into aged mice on microglia, sections of poststroke brain were stained with anti-Iba-1 antibody. Compared with PBS-treated rats (Figure 5L), a significant decrease in microglia was observed in the peristroke area in bone marrow transplanted rats versus nontransplanted animals (Figures 5M and 5N). In contrast, no significant difference was observed in the number of microglia in the contralateral cortex comparing PBS-treated rats and bone marrow transplanted rats (29.1 ± 1.6 and 27.2 ± 1.7/field, respectively; $P = 0.45$).

Discussion

We have demonstrated that partial rejuvenation of bone marrow from aged rats with bone marrow-derived mononuclear cells from young animals reduces damage after experimental cerebral ischemia in the SHR-SP rat strain.

Intravenous infusion of bone marrow-derived cells without pretreatment for transplantation (such as irradiation) is associated with a very low seeding efficiency of transplanted cells into host bone marrow. However, pretransplant radiation of individuals not requiring complete repopulation of bone marrow with transplanted cells (as would be true for patients with cerebral ischemia, especially during the immediate period of ischemic stress) is not likely to be clinically acceptable, due to short- and long-term complications. Thus, use of intrabone marrow administration of bone marrow-derived mononuclear cells, in addition to intravenous administration of bone marrow cells, was used for our studies. Using our protocol (i.e., no pretreatment for bone marrow transplantation, followed by intravenous and intrabone marrow administration of bone marrow cells), the level of engraftment resulted in $\approx 5\%$ chimera of transplanted versus host cells in peripheral blood. Furthermore, analysis of peripheral blood from transplanted animals showed no significant difference in mature cell populations between the two groups. Although the overall change in health status of the aged rats because of transplantation of bone marrow cells is difficult to evaluate, these results indicate that the beneficial effect of transplanting bone marrow-derived mononuclear cells from young SHR-SP into old animals, in terms of limiting brain injury following ischemia, is not simply due to optimization of the level of circulating mature cells.

Initially, we suspected that our bone marrow transplant protocol would result in a change in the cytokine response to cerebral ischemia consistent with diminished inflammation and enhanced repair. However, levels of IL-1β and MCP-1, considered deleteriously inflammatory (Chen *et al*, 2003; Holmin and Mathiesen, 2000), increased (Figure 3), and levels of IL-6, considered protective (Loddick *et al*, 1998), was not increased (Figure 3), following bone marrow transplantation. These findings indicate that beneficial effects of transplanting young

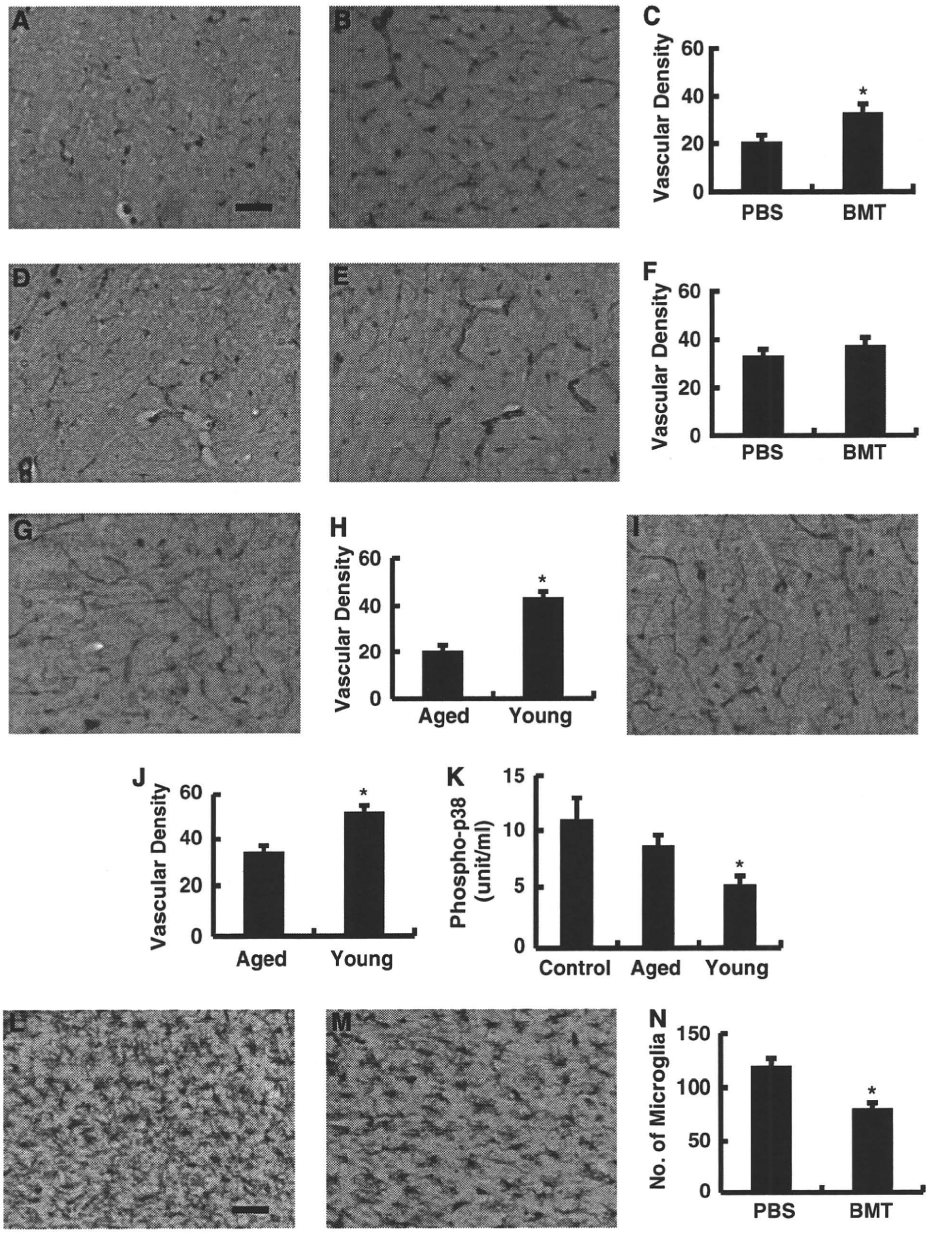

Figure 5 Effect of bone marrow transplanted (BMT) using bone marrow from young animals into aged animals on the density of vascular structures in the periinfarction area during the poststroke period. (**A–C**) Representative micrographs of cerebral cortex about 0.5 mm from the stroke-affected area in the phosphate-buffered saline (PBS) (**A**) and BMT (**B**) groups on day 30 after stroke. Sections were stained with anti-Lectin antibody. There is a significant difference in vascular density observed between groups (**C**). (**D–F**) Representative micrographs of contralateral cortex in the PBS (**D**) and BMT (**E**) groups on day 30 after stroke. No significant difference in vascular density was observed between the two groups (**F**). (**G–J**) Representative micrograph of ipsilateral stroke-affected cortex (**G**) and contralateral cortex (**I**) of a poststroke young rat on day 30 after stroke. Compared with aged rats subjected to stroke, there is a significant increase in vascular density in the stroke-affected cortex located about 0.5 mm from the stroke area (**H**) and contralateral cortex (**J**) in the young animals. (**K**) Human umbilical vein endothelial cells (HUVECs) were exposed to bone marrow mononuclear cells from aged or young rats and the level of endothelial cell phospho-p38 was determined. Analysis of variance analysis revealed a significant reduction in endothelial phospho-p38 in the presence of young bone marrow cells compared with aged bone marrow cells. (**L–N**) Representative micrographs of cerebral cortex about 0.5 mm from the stroke-affected area from an animal in the PBS (**L**) and BMT (**M**) group on day 30 after stroke. The section is stained with anti-Iba-1 antibody. A significant reduction in microglia was observed in the BMT group, compared with PBS-treated group (**N**). $*P < 0.05$ versus PBS control (**C**, **N**) or aged bone marrow (**H**, **J**, **K**). $n = 5$, in each group. Scale bar: 50 μm (**A**, **L**).

bone marrow into aged animals are not likely due to modulating the profile of inflammatory cytokines at the site of cerebral infarction or in the serum.

Vascular endothelial dysfunction in aging has been shown to be correlate with impaired vasodilatation (LeBlanc *et al*, 2008) and reduced expression of NOS

(Smith and Hagen, 2003). Although some aspects of cell senescence are likely to be irreversible, certain endothelial properties can be maintained/restored with antioxidants (Smith and Hagen, 2003). Furthermore, exposure to a 'young systemic environment' has been shown to rejuvenate aged progenitor cells in rats (Conboy *et al*, 2005). Taken together with these previous observations, our results indicate that partial reconstitution of bone marrow from aged rats with cells from young animals improves the host response to cerebral ischemia, probably in part through a beneficial effect on endothelial function. Although bone marrow cells have the potential to differentiate into endothelial cells (Asahara *et al*, 1997), the half-life of endothelial cells is relatively long and differentiation of circulating cells into endothelium is relatively rare (Taguchi *et al*, 2004*b*). Thus, the principal effect of young progenitors in the bone marrow may be to promote an environment in the systemic circulation conducive to vascular activation, as evidenced by increased levels of phospho-eNOS (i.e., the results of our *in vitro* studies with cultured HUVEC exposed to mononuclear bone marrow cells from young versus old rats; Figure 4E). In addition to eNOS, young bone marrow cells were shown to decrease activation of p38 MAP kinase in cultured endothelium, a pathway leading to cell death (Mehta *et al*, 2007). In contrast, no significant change in activation/inactivation of other MAP kinases, ERK1/2 or JNK, was observed in endothelial cells exposed to bone marrow cells from young animals *in vitro*. In a previous report, inactivation of p38, but not JNK, was shown to suppress endothelial cell death after hypoxia/reoxygenation injury (Lee and Lo, 2003). Taken together, our data thus far suggests that the beneficial effect of bone marrow cells from young animals may be due, at least in part, to effects on the vascular endothelium, especially at the level of cerebral microvasculature. This concept is consistent with our observation of an increased density of vascular structures in the periinfarct area of poststroke brain from aged rats transplanted with bone marrow cells from young animals. However, the precise mechanisms linking bone marrow-derived immature cells to enhanced function of the cerebral microcirculation remains to be determined (Pearson, 2009). In view of the likely impact of inflammatory mechanisms on reparative mechanisms in stroke, another important observation might be the decrease of microglial invasion/activation observed in poststroke aged animals transplanted with bone marrow from young animals.

Our results suggest a novel strategy for enhancing the host response to ischemia in aged patients, provided these observations in a rodent model can be translated to humans. If such an extrapolation to man is possible, the source of 'young' bone marrow is relatively easily obtained through collection and preservation of autologous cord blood or bone marrow cells harvested earlier in life. In addition, an alternative approach might be induction of hematopoietic stem cells using autologous induced pluripotent stem (iPS) cells (Hanna *et al*, 2007). Although the fundamental mechanisms underlying senescence of mammalian cells (and senescence of the vasculature) remains to be elucidated, our findings indicate that impairment of the vascular response in aged individuals may be partially restored through transplantation with bone marrow from young animals. In addition to possible therapeutic application in patients with an evolving stroke, rejuvenation of bone marrow may also have a preventive role in those at high risk for stroke, such as individuals with recurrent transient ischemic attacks.

Disclosure/conflict of interest

The authors declare no conflict of interest.

References

Asahara T, Murohara T, Sullivan A, Silver M, van der Zee R, Li T, Witzenbichler B, Schatteman G, Isner JM (1997) Isolation of putative progenitor endothelial cells for angiogenesis. *Science* 275:964–7

Brandle M, al Makdessi S, Weber RK, Dietz K, Jacob R (1997) Prolongation of life span in hypertensive rats by dietary interventions. Effects of garlic and linseed oil. *Basic Res Cardiol* 92:223–32

Chen Y, Hallenbeck JM, Ruetzler C, Bol D, Thomas K, Berman NE, Vogel SN (2003) Overexpression of monocyte chemoattractant protein 1 in the brain exacerbates ischemic brain injury and is associated with recruitment of inflammatory cells. *J Cereb Blood Flow Metab* 23: 748–55

Conboy IM, Conboy MJ, Wagers AJ, Girma ER, Weissman IL, Rando TA (2005) Rejuvenation of aged progenitor cells by exposure to a young systemic environment. *Nature* 433:760–4

Farkas T, Racekova E, Kis Z, Horvath S, Burda J, Galik J, Toldi J (2003) Peripheral nerve injury influences the disinhibition induced by focal ischaemia in the rat motor cortex. *Neurosci Lett* 342:49–52

Hanna J, Wernig M, Markoulaki S, Sun CW, Meissner A, Cassady JP, Beard C, Brambrink T, Wu LC, Townes TM, Jaenisch R (2007) Treatment of sickle cell anemia mouse model with iPS cells generated from autologous skin. *Science* 318:1920–3

Hill JM, Zalos G, Halcox JP, Schenke WH, Waclawiw MA, Quyyumi AA, Finkel T (2003) Circulating endothelial progenitor cells, vascular function, and cardiovascular risk. *N Engl J Med* 348:593–600

Holmin S, Mathiesen T (2000) Intracerebral administration of interleukin-1beta and induction of inflammation, apoptosis, and vasogenic edema. *J Neurosurg* 92:108–20

Hutchins PM, Lynch CD, Cooney PT, Curseen KA (1996) The microcirculation in experimental hypertension and aging. *Cardiovasc Res* 32:772–80

Inaba M, Adachi Y, Hisha H, Hosaka N, Maki M, Ueda Y, Koike Y, Miyake T, Fukui J, Cui Y, Mukaide H, Koike N, Omae M, Mizokami T, Shigematsu A, Sakaguchi Y, Tsuda M, Okazaki S, Wang X, Li Q, Nishida A, Ando Y, Guo K, Song C, Cui W, Feng W, Katou J, Sado K, Nakamura S, Ikehara S (2007) Extensive studies on

perfusion method plus intra-bone marrow-bone marrow transplantation using cynomolgus monkeys. *Stem Cells* 25:2098–103

Kamihata H, Matsubara H, Nishiue T, Fujiyama S, Tsutsumi Y, Ozono R, Masaki H, Mori Y, Iba O, Tateishi E, Kosaki A, Shintani S, Murohara T, Imaizumi T, Iwasaka T (2001) Implantation of bone marrow mononuclear cells into ischemic myocardium enhances collateral perfusion and regional function via side supply of angioblasts, angiogenic ligands, and cytokines. *Circulation* 104:1046–52

Kant S, Schumacher S, Singh MK, Kispert A, Kotlyarov A, Gaestel M (2006) Characterization of the atypical MAPK ERK4 and its activation of the MAPK-activated protein kinase MK5. *J Biol Chem* 281:35511–9

Kasahara Y, Taguchi A, Uno H, Nakano A, Nakagomi T, Hirose H, Stern DM, Matsuyama T (2010) Telmisartan suppresses cerebral injury in a murine model of transient focal ischemia. *Brain Res* 1340:70–80

LeBlanc AJ, Shipley RD, Kang LS, Muller-Delp JM (2008) Age impairs Flk-1 signaling and NO-mediated vasodilation in coronary arterioles. *Am J Physiol Heart Circ Physiol* 295:H2280–8

Lee SR, Lo EH (2003) Interactions between p38 mitogen-activated protein kinase and caspase-3 in cerebral endothelial cell death after hypoxia-reoxygenation. *Stroke* 34:2704–9

Li C, He Y, Feng X, Inaba M, Adachi Y, Takada K, Zhang Y, Yamamoto Y, Wu X, Cui Y, Iwasaki M, Hisha H, Hosaka N, Taira M, Minamino K, Suzuki Y, Nakano K, Fukui J, Ueda Y, Koike Y, Tsuda M, Ikehara S (2007) An innovative approach to bone marrow collection and transplantation in a patient with beta-thalassemia major: marrow collection using a perfusion method followed by intra-bone marrow injection of collected bone marrow cells. *Int J Hematol* 85:73–7

Loddick SA, Turnbull AV, Rothwell NJ (1998) Cerebral interleukin-6 is neuroprotective during permanent focal cerebral ischemia in the rat. *J Cereb Blood Flow Metab* 18:176–9

Lynch CD, Cooney PT, Bennett SA, Thornton PL, Khan AS, Ingram RL, Sonntag WE (1999) Effects of moderate caloric restriction on cortical microvascular density and local cerebral blood flow in aged rats. *Neurobiol Aging* 20:191–200

Majka M, Janowska-Wieczorek A, Ratajczak J, Ehrenman K, Pietrzkowski Z, Kowalska MA, Gewirtz AM, Emerson SG, Ratajczak MZ (2001) Numerous growth factors, cytokines, and chemokines are secreted by human CD34(+) cells, myeloblasts, erythroblasts, and megakaryoblasts and regulate normal hematopoiesis in an autocrine/paracrine manner. *Blood* 97:3075–85

Meaney MJ, O'Donnell D, Rowe W, Tannenbaum B, Steverman A, Walker M, Nair NP, Lupien S (1995) Individual differences in hypothalamic-pituitary-adrenal activity in later life and hippocampal aging. *Exp Gerontol* 30:229–51

Mehta SL, Manhas N, Raghubir R (2007) Molecular targets in cerebral ischemia for developing novel therapeutics. *Brain Res Rev* 54:34–66

Pearce DJ, Anjos-Afonso F, Ridler CM, Eddaoudi A, Bonnet D (2007) Age-dependent increase in side population distribution within hematopoiesis: implications for our understanding of the mechanism of aging. *Stem Cells* 25:828–35

Pearson JD (2009) Endothelial progenitor cells—hype or hope? *J Thromb Haemost* 7:255–62

Schmidt-Lucke C, Rossig L, Fichtlscherer S, Vasa M, Britten M, Kamper U, Dimmeler S, Zeiher AM (2005) Reduced number of circulating endothelial progenitor cells predicts future cardiovascular events: proof of concept for the clinical importance of endogenous vascular repair. *Circulation* 111:2981–7

Smith AR, Hagen TM (2003) Vascular endothelial dysfunction in aging: loss of Akt-dependent endothelial nitric oxide synthase phosphorylation and partial restoration by (R)-alpha-lipoic acid. *Biochem Soc Trans* 31:1447–9

Sonntag WE, Lynch CD, Cooney PT, Hutchins PM (1997) Decreases in cerebral microvasculature with age are associated with the decline in growth hormone and insulin-like growth factor 1. *Endocrinology* 138:3515–20

Sullivan PG, Bruce-Keller AJ, Rabchevsky AG, Christakos S, Clair DK, Mattson MP, Scheff SW (1999) Exacerbation of damage and altered NF-kappaB activation in mice lacking tumor necrosis factor receptors after traumatic brain injury. *J Neurosci* 19:6248–56

Taguchi A (2009) Vascular factors in diabetes and Alzheimer's disease. *J Alzheimers Dis* 16:859–64

Taguchi A, Matsuyama T, Moriwaki H, Hayashi T, Hayashida K, Nagatsuka K, Todo K, Mori K, Stern DM, Soma T, Naritomi H (2004*a*) Circulating CD34-positive cells provide an index of cerebrovascular function. *Circulation* 109:2972–5

Taguchi A, Matsuyama T, Nakagomi T, Shimizu Y, Fukunaga R, Tatsumi Y, Yoshikawa H, Kikuchi-Taura A, Soma T, Moriwaki H, Nagatsuka K, Stern DM, Naritomi H (2008) Circulating CD34-positive cells provide a marker of vascular risk associated with cognitive impairment. *J Cereb Blood Flow Metab* 28:445–9

Taguchi A, Nakagomi N, Matsuyama T, Kikuchi-Taura A, Yoshikawa H, Kasahara Y, Hirose H, Moriwaki H, Nakagomi T, Soma T, Stern DM, Naritomi H (2009) Circulating CD34-positive cells have prognostic value for neurologic function in patients with past cerebral infarction. *J Cereb Blood Flow Metab* 29:34–8

Taguchi A, Ohtani M, Soma T, Watanabe M, Kinosita N (2003) Therapeutic angiogenesis by autologous bone-marrow transplantation in a general hospital setting. *Eur J Vasc Endovasc Surg* 25:276–8

Taguchi A, Soma T, Tanaka H, Kanda T, Nishimura H, Yoshikawa H, Tsukamoto Y, Iso H, Fujimori Y, Stern DM, Naritomi H, Matsuyama T (2004*b*) Administration of CD34+ cells after stroke enhances neurogenesis via angiogenesis in a mouse model. *J Clin Invest* 114:330–8

Taguchi A, Wen Z, Myojin K, Yoshihara T, Nakagomi T, Nakayama D, Tanaka H, Soma T, Stern DM, Naritomi H, Matsuyama T (2007) Granulocyte colony-stimulating factor has a negative effect on stroke outcome in a murine model. *Eur J Neurosci* 26:126–33

Tateishi-Yuyama E, Matsubara H, Murohara T, Ikeda U, Shintani S, Masaki H, Amano K, Kishimoto Y, Yoshimoto K, Akashi H, Shimada K, Iwasaka T, Imaizumi T (2002) Therapeutic angiogenesis for patients with limb ischaemia by autologous transplantation of bone-marrow cells: a pilot study and a randomised controlled trial. *Lancet* 360:427–35

Watson JV, Nakeff A, Chambers SH, Smith PJ (1985) Flow cytometric fluorescence emission spectrum analysis of Hoechst-33342-stained DNA in chicken thymocytes. *Cytometry* 6:310–5

Werner N, Kosiol S, Schiegl T, Ahlers P, Walenta K, Link A, Bohm M, Nickenig G (2005) Circulating endothelial

progenitor cells and cardiovascular outcomes. *N Engl J Med* 353:999–1007

Yamahara K, Sone M, Itoh H, Yamashita JK, Yurugi-Kobayashi T, Homma K, Chao TH, Miyashita K, Park K, Oyamada N, Sawada N, Taura D, Fukunaga Y, Tamura N, Nakao K (2008) Augmentation of neovascularization in hindlimb ischemia by combined transplantation of human embryonic stem cells-derived endothelial and mural cells. *PLoS One* 3:e1666

Yang GY, Gong C, Qin Z, Ye W, Mao Y, Bertz AL (1998) Inhibition of TNFalpha attenuates infarct volume and ICAM-1 expression in ischemic mouse brain. *Neuroreport* 9:2131–4

Yoshihara T, Taguchi A, Matsuyama T, Shimizu Y, Kikuchi-Taura A, Soma T, Stern DM, Yoshikawa H, Kasahara Y, Moriwaki H, Nagatsuka K, Naritomi H (2008) Increase in circulating CD34-positive cells in patients with angiographic evidence of moyamoya-like vessels. *J Cereb Blood Flow Metab* 28:1086–9

Zhang B, Hata R, Zhu P, Sato K, Wen TC, Yang L, Fujita H, Mitsuda N, Tanaka J, Samukawa K, Maeda N, Sakanaka M (2006) Prevention of ischemic neuronal death by intravenous infusion of a ginseng saponin, ginsenoside Rb(1), that upregulates Bcl-x(L) expression. *J Cereb Blood Flow Metab* 26:708–21

Published in final edited form as:
J Exp Stroke Transl Med. 2010 March ; 3(1): 28–33.

A Reproducible and Simple Model of Permanent Cerebral Ischemia in CB-17 and SCID Mice

Akihiko Taguchi, MD[1], **Yukiko Kasahara**[1], **Takayuki Nakagomi, MD**[2], **David M. Stern, MD**[3], **Mari Fukunaga**[4], **Makoto Ishikawa, PhD**[4], and **Tomohiro Matsuyama, MD**[2]

[1]Department of Cerebrovascular Disease, National Cardiovascular Center, Osaka, Japan

[2]Institute for Advanced Medical Sciences, Hyogo College of Medicine, Hyogo, Japan

[3]VPHA and Dean's Office, College of Medicine, University of Cincinnati, OH, USA

[4]Laboratory of Bioenergetics Research, Tokushima Research Institute, Otsuka Pharmaceutical Co, Ltd. Tokushima, Japan

Abstract

In order to evaluate novel stroke therapies, it is essential to utilize a highly reproducible model of focal cerebral ischemia. Though a range of rodent stroke models has been employed in the literature, there are persistent issues regarding reproducibility of the ischemic zone, as there is considerable inter-animal and inter-laboratory variation. We have developed a highly reproducible model of stroke that involves direct electrocoagulation of the MCA in SCID (CB-17/Icr-scid/scidJcl) and CB-17 (CB-17/Icr-+/+Jcl) mice. Using a modification of the Tamura method, our results demonstrate reproducible cortical infarction with high survival in the chronic period (up to 180 days) in SCID and CB-17, but not in C57BL/6, mice. We believe that our preclinical model represents a step forward for testing future therapeutic methods potentially applicable to patients with stroke.

Keywords

stroke model; permanent cerebral ischemia; reproducibility

Introduction

A range of stroke models has been developed to simulate clinically relevant subtypes of stroke (Liu *et al.* 2009). Focal cerebral ischemia has been used to model ischemic stroke, and the Tamura(Tamura *et al.* 1981) and intraluminal filament models(Longa *et al.* 1989) have been employed most commonly. A key issue in the evaluation of data obtained in these models concerns reproducibility of the stroke-affected region and the survival rate of animals during the chronic period. Various modifications of the latter methods have been employed to address these issues(Chen *et al.* 1986; Hirakawa *et al.* 1994; Kuge *et al.* 1995).

Because murine models are preferable for screening new therapies, though vascular structures in mice can demonstrate inter-strain variability, we have assessed the reproducibility of the

Correspondence should be addressed to: A.T. and T.M. AKIHIKO TAGUCHI: taguchi@ri.ncvc.go.jp, Department of Cerebrovascular Disease, National Cardiovascular Center, 5-7-1 Fujishiro-dai, Suita, Osaka, Japan, 565-8565, Phone: +81-6-6833-5012 Fax: +81-6-6872-7485, TOMOHIRO MATSUYAMA : tomohiro@hyo-med.ac.jp, Institute for Advanced Medical Sciences, Hyogo College of Medicine, 1-1 Mukogawacho, Nishinomiya, Hyogo, Japan, 663-8501, Phone +81-798-45-6822 Fax +81-798-45-6823.

Disclosure / Conflict of interest
The authors indicate no potential conflicts of interest.

stroke-affected area in different strains by simple direct ligation of the MCA. We have found that ligation of the distal portion of the MCA in SCID or CB-17 mice induces reproducible and selective cortical infarction. In previous reports, we have outlined our stroke model in SCID(Nakagomi *et al.* 2009; Taguchi *et al.* 2004) and CB-17(Taguchi *et al.* 2007) mice. In this manuscript, we provide the detailed methods, allowing for easy replication of our work, and discuss the advantages and limitations of our model.

Materials and Methods

All procedures were performed under auspices of an approved protocol from the National Cardiovascular Center Animal Care and Use Committee.

Induction of Permanent Focal Cerebral Ischemia

Male SCID (CB-17/lcr-scid/scidJcl), CB-17 (CB-17/lcr-+/+Jcl) and C57BL/6 (C57BL/6NJcl) mice were purchased from Clea Japan (Tokyo, Japan). Animals were allowed access to food and tap water *ad libitum*. Powdered chow and sterilized water were also provided during the first 7 days after induction of stroke.

Cerebral infarction was studied in 8 week-old mice according to a modification of the Tamura method. General anesthesia was induced and maintained by inhalation of 3% and 1.5% halothane (7025 Rodent Ventilator, Ugo Basile, Italy), respectively. Mice were oriented as indicated, and a skin incision was made between left eyeball and left ear hole (Figure 1A). The left salivary gland and veins were carefully removed to visualize the zygoma. The left zygoma was dissected under an operating microscope (KOM300S, Konan Medical, Nishinomiya, Japan), and the jaw joint was detached to allow visualization of the MCA through the cranial bone. A hole (diameter, 1.5 mm) was made in the bone using a dental drill (C710, Senko Medical Instrument Manufacturing, Tokyo, Japan). Subsequently, the dura matter was carefully removed with caution not to damage the surface of the brain. Then, the MCA was isolated (Figure 1B, lower magnification; C, higher magnification), electrocauterized (Figure 1D) and disconnected distal to crossing the olfactory tract (distal M1 portion, Figure 1E). It is notable that very mild and gradual coagulation is required in order for electrocoagulation to avoid bleeding from the MCA. We used an electrocoagulator designed for ophthalmologic surgery (MERA MS-50, Senko Medical Instrument, Tokyo, Japan) and the bipolar forceps (MERA NF-14) at an output level of 1.0 Watt. Sequential, very brief coagulation with the top of the bipolar forceps is recommended, starting from the distal portion of MCA to the proximal portion. Repetition of this procedure, usually 2 to 4 times, stopped blood flow in the vessel. After that, the MCA was coagulated from the distal to the proximal portion. This method resulted in a very low risk of bleeding from the MCA.

Cerebral blood flow (CBF) in the MCA area was monitored as described(Taguchi *et al.* 2007). Briefly, an acrylate column (Neuroscience Co., Ltd., Osaka, Japan) was attached to the intact skull using stereotactic coordinates (1 mm anterior and 3 mm lateral to the bregma), and CBF was monitored using a linear probe (1 mm in diameter) by laser Doppler flowmetry (Neuroscience Co., Ltd.). Body temperature was maintained at 36.5–37°C using a heat lamp and animal blanket controller (ATB-1100, Nipponkoden,Tokyo, Japan) during the operation.

Evaluation of Stroke Volume

Twenty-four hours after induction of stroke, the area subject to ischemic damage was evaluated by 7T MRI (N=8; Inova 300 Imaging System; Varian, Inc., Palo Alto, CA. USA). The volume coil for RF excitation was actively decoupled and used in combination with a fixed tuned and matched receiver surface coil (Rapid Biomedical GmbH, Germany) that was placed over the skull. For MRI measurements, mice were placed in a stereotactic head holder and anesthetized

with 2.0–2.5% halothane in a mixture of O_2 and N_2O gas delivered through a facemask. The fraction of inspired oxygen (FiO_2) was adjusted to 30%. Rectal temperature was feedback-controlled at 37.5 ± 0.5°C using warm air. T2 images were obtained by a multislice spin echo sequence. Parameters included: TR = 3000 ms; TE = 10, 30, 50, 70 and 90 ms; and, NS = 1. Slice thickness was 1 mm, matrix size was 256 × 128, and images were zero-filled to 256 × 256. The field of view was 30 mm × 30 mm. MR image analysis employed the image browser (VNMR 6.1C and Solaris 7, Varian, Inc., Palo Alto, CA, USA). Lesion area in T2 images was calculated as the region with T2 above T2+3SD of each contralateral value. Ischemia-affected volumes from MR images were calculated by summing lesion areas in 7 slices and multiplying by slice thickness (1 mm). Percent ischemia-affected volume was calculated according to (ischemia affected volume) / [(contralateral cortex volume) × 2] × 100%.

Twenty-six (SCID; N=8) or 24 (CB-17; N=8 and C57BL/6; N=8) hours after stroke, viability of brain tissue was evaluated using 1% 2,3,5-triphenyltetrazolium (TTC; Sigma-Aldrich, St. Louis, MO, USA) for 20 min at 37°C. Tissues were then fixed in 4% paraformaldehyde/ phosphate-buffered saline (PBS; pH 7.4). Images of sections were captured using a microscopic digital camera system and % stroke volume was estimated with an image analysis program (BZ-2: Keyence, Osaka, Japan) which compared data in the stroke-affected hemisphere to that in the contralateral hemisphere. As with MRI images, % stroke volume was calculated by (stroke volume) / [(contralateral cortex volume) × 2] × 100 %.

Data Analysis

In all experiments, mean ± standard deviation is reported. JMP 7.01 (SAS Institute Inc, Co, North Carolina, USA) was used for statistical analysis.

Results

Stroke Model in SCID Mice

Cerebral infarction was induced by direct electrocoagulation of the distal portion of the MCA in SCID mice. In the current experiment, we used 8 mice and all animals displayed vascular structures with either one major MCA without other visible cortical branches (Figure 1E, N=5) or with just one significantly thinner cortical branch (Figure 1B, N=3) in the M1 distal portion of the MCA. The main trunk of the MCA was electrocauterized (Figure 1C) and disconnected (Figure 1D). Twenty-four hours after induction of permanent ischemia, brain damage was evaluated by T2-weighted MRI (all of the images are shown in Figure 2). Our results demonstrate that the mean % schemia-affected volume was 17.1 ± 1.4% and the variation coefficient was 7.8%.

To assess viability of the cerebral cortex following ischemia, brain sections were stained with TTC 26 hours after stroke. Similar to MRI images, highly reproducible cerebral damage was observed between animals and the mean % stroke volume and variation coefficient were 14.9 ± 1.0 % and 6.6 %, respectively.

Before and after ligation of the MCA, the change in CBF in the cerebral cortex in the MCA area was evaluated using laser Doppler. Compared with before stroke, mean CBF decreased to 17.9 ± 5.0 and 19.7 ± 3.9 %, immediately and 5 minutes after induction of stroke, respectively. Comparing % viable ipsilateral cerebral volume and decreased CBF showed no significant correlation between size of the subsequent infarct and CBF immediately (R^2=0.05, P=0.61) and 5 minutes (R^2=0.08, P=0.48) after induction of ischemia.

To access the survival in the chronic period, 16 mice were induced cerebral infarction. The survival rate at 90 and 180 days after induction of stroke was 100 (16/16) and 94 (15/16) %, respectively.

Stroke Model in CB-17 Mice

Similarly, cerebral ischemia was induced in CB-17 mice (N=8). Twenty-four hours after induction of cerebral ischemia, stroke area was evaluated by TTC staining (representative images are shown in Figure 3A,B). Mean stroke volume was 14.3 ± 0.9 %, and variation coefficient was 6.3 %. Compared with before stroke, mean CBF decreased to 18.1 ± 3.1 and 20.0 ± 4.2 %, immediately and 5 minutes after induction of stroke, respectively. There was no significant correlation between the size of infarction and CBF immediately (R^2=0.001, P=0.94) and 5 minutes (R^2=0.02, P=0.73) after induction of stroke. It is notable that a small TTC-negative area was observed around the immediate area of coagulation of the MCA (Figure 3). As a control, brain sections from sham-operated mice were also stained with TTC. In contrast, no defect in TTC staining was observed in the controls at the 24 hr point after induction of stroke (not shown).

Survival at 180 days after induction of stroke was 100 (16/16) % (N=16).

Stroke Model in C57BL/6 Mice

As a control, we induced cerebral ischemia in C57BL/6 mice (N=8) by ligation of the M1 distal portion of the main trunk of the MCA. Only 4 mice showed decreased CBF to less than 25% compared with the baseline before ligation. Twenty-four hours after induction of permanent ischemia, stroke area in these 4 mice was evaluated by TTC staining (representative images are shown in Figure 3C–D). Mean stroke volume was 5.0 ± 3.2 %, and the variation coefficient was 63.4%.

Discussion

In this article, we have demonstrated that ligation of the distal portion of the MCA in SCID and CB-17 mice, using a modification of the Tamura method, induces highly reproducible and selective cortical infarction.

The advantages of this method include: a) the model produces very reproducible areas of cortical infarction, allowing for effective screening of various experimental treatments using smaller numbers of mice; b) because of its simplicity, the method is broadly accessible to a wide range of investigators; c) the long-term survival rate (up to 180 days) is high, allowing assessment of therapeutic and/or side effects of experimental treatments during the chronic period; d) as a model of focal permanent ischemia, the model mimics, in part, human cerebral infarction; e) CB-17 and SCID mice are easy to procure and require no special diet or pre-treatment regimen; f) use of SCID mice allows evaluation of cell-based therapies with donor cells from different species/strains; and, g) reproducible stroke area is observed during the chronic period(Taguchi *et al.* 2004; Taguchi *et al.* 2007) and the latter corresponds to the TTC-negative area observed 24 hours after induction of stroke.

Of course, there are also short-comings of our model: a) there are few transgenic/knockout mice in CB-17 strain, so animals must be bred into that background; b) craniotomy results in stress to the overall animal and trauma to local tissues; and, c) our model results in minimal motor dysfunction accompanying focal ischemia. We have demonstrated that the open field test a reliable and simple test of cortical function after stroke in this model(Taguchi *et al.* 2004; Taguchi *et al.* 2007). However, further investigation will be needed for a complete evaluation of cortical function.

According to our previous experiments, most SCID and CB-17 mice displayed the same vascular structures/organization. Though the great majority of mice showed highly reproducible stroke area, 1.1 % (4/362) of SCID and 4.9% (6/122) of CB-17 mice displayed an expanded area extending across the corpus callosum to the striatum. Expansion of the stroke-

affected was rarely observed in mice with a thin cortical branch, but was frequently observed in mice with a major cortical branch. These observations suggest that evaluation of MCA branching in a range of mouse strains might provide a means of increasing the reproducibility of other stroke models. To reduce variability using our method of focal cerebral ischemia, we recommend excluding from the experimental protocol mice with major variations in MCA structure, such as changes in the width of the cortical branch artery (branched before olfactory tract) especially when this represents more than one-third that of the main trunk.

In our experiments, all mice showed significant reduction (less than 25%, compared with before ligation) of CBF by ligation of the MCA, and no significant correlation was observed between decreased CBF after the procedure and subsequent stroke volume. Furthermore, no significant correlation was observed between decreased CBF and cortical function in our previous work (Taguchi *et al.* 2004). These data indicate that determination of CBF in this model may not be especially important for initial screening of various treatments after stroke. If the investigator excludes measurement of CBF, all procedures can be finished within 15 minutes when the method is performed by experienced hands. The latter should facilitate screening multiple drugs or other types of interventions.

In conclusion, our focal permanent cerebral ischemia model using SCID and CB-17 mice provides a reproducible method for induction of cerebral infarction, results in high long-term survival, and employs a relatively simple procedure. Though we have not confirmed the level of inter-lab variation, especially outside of Japan, where SCID and CB-17 mice might display greater variability in cerebral vascular structure, our findings provide, we believe, a new strategy for evaluating potential future therapeutic methods for the benefit of patients with stroke.

Acknowledgments

This work was supported by a Research Grant for Cardiovascular Diseases (21A-7) from the Ministry of Health, Labour and Welfare.

References

Chen ST, Hsu CY, Hogan EL, Maricq H, Balentine JD. A model of focal ischemic stroke in the rat: reproducible extensive cortical infarction. Stroke 1986;17:738–743. [PubMed: 2943059]

Hirakawa M, Tamura A, Nagashima H, Nakayama H, Sano K. Disturbance of retention of memory after focal cerebral ischemia in rats. Stroke 1994;25:2471–2475. [PubMed: 7974591]

Kuge Y, Minematsu K, Yamaguchi T, Miyake Y. Nylon monofilament for intraluminal middle cerebral artery occlusion in rats. Stroke 1995;26:1655–1657. discussion 1658. [PubMed: 7660413]

Liu S, Zhen G, Meloni B, Campbell K, Winn H. Rodent stroke model guidlines for preclinical stroke trials (1st edtiton). J Exp Stroke Transl Med 2009;2:2–27. [PubMed: 20369026]

Longa EZ, Weinstein PR, Carlson S, Cummins R. Reversible middle cerebral artery occlusion without craniectomy in rats. Stroke 1989;20:84–91. [PubMed: 2643202]

Nakagomi N, Nakagomi T, Kubo S, Nakano-Doi A, Saino O, Takata M, Yoshikawa H, Stern DM, Matsuyama T, Taguchi A. Endothelial cells support survival, proliferation, and neuronal differentiation of transplanted adult ischemia-induced neural stem/progenitor cells after cerebral infarction. Stem Cells 2009;27:2185–2195. [PubMed: 19557831]

Taguchi A, Soma T, Tanaka H, Kanda T, Nishimura H, Yoshikawa H, Tsukamoto Y, Iso H, Fujimori Y, Stern DM, Naritomi H, Matsuyama T. Administration of CD34+ cells after stroke enhances neurogenesis via angiogenesis in a mouse model. J Clin Invest 2004;114:330–338. [PubMed: 15286799]

Taguchi A, Wen Z, Myojin K, Yoshihara T, Nakagomi T, Nakayama D, Tanaka H, Soma T, Stern DM, Naritomi H, Matsuyama T. Granulocyte colony-stimulating factor has a negative effect on stroke outcome in a murine model. Eur J Neurosci 2007;26:126–133. [PubMed: 17614944]

Tamura A, Graham DI, McCulloch J, Teasdale GM. Focal cerebral ischaemia in the rat: 1. Description of technique and early neuropathological consequences following middle cerebral artery occlusion. J Cereb Blood Flow Metab 1981;1:53–60. [PubMed: 7328138]

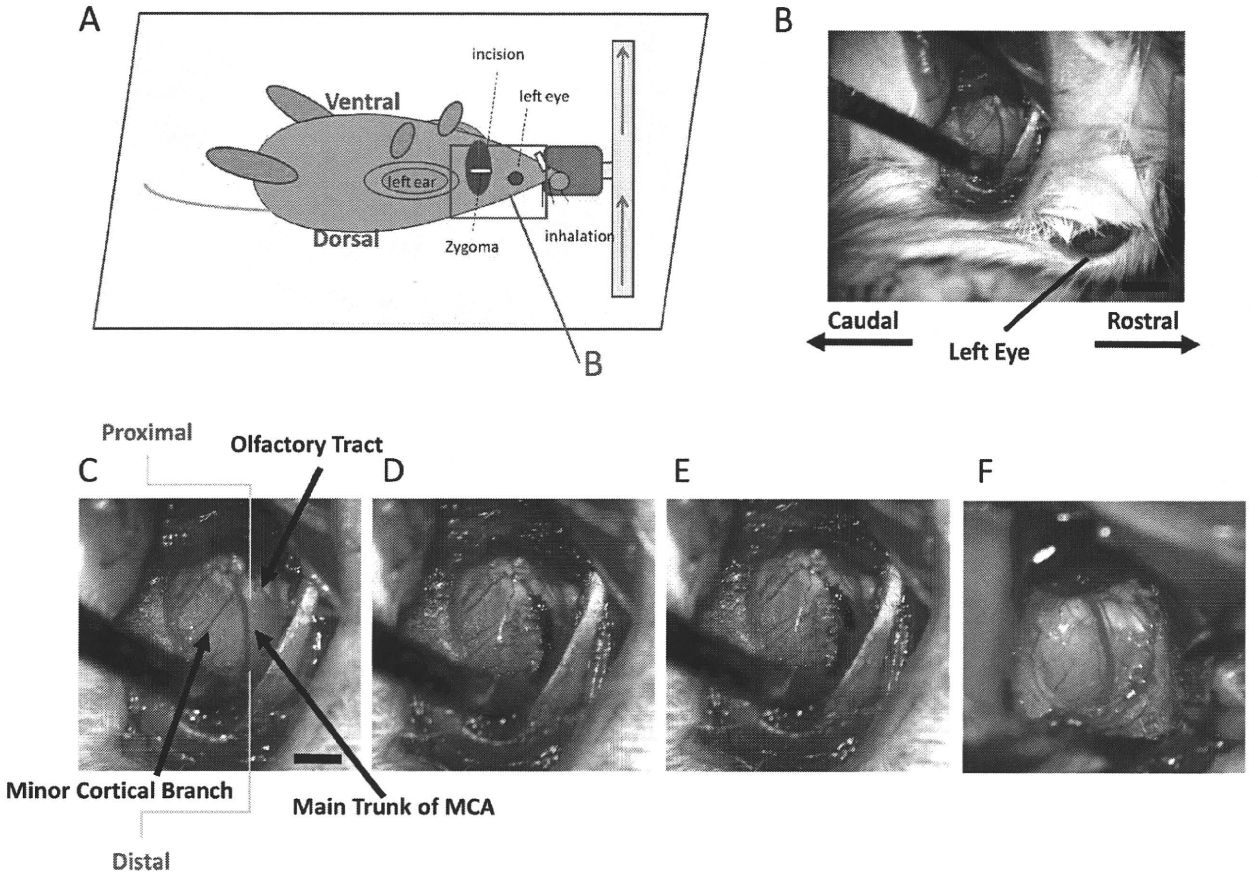

Figure 1. Ligation of the distal portion of MCA

(A) Schematic depiction showing orientation of the animal in our model for induction of stroke. The red rectangle represents the portion shown in panel B. (B–E) After dissecting the left zygoma, a hole was made and the dura was carefully removed (B; lower magnification, C; higher magnification). The main trunk of the MCA was electrocoagulated (D) and disconnected using the tip of 30G needle (E). This mouse had a minor cortical branch (C), but electrocoagulation and disconnection of main trunk resulted in disappearance of blood flow in the minor cortical branch. Panel (F) shows a representative picture of the vascular structure without a minor cortical branch around olfactory tract. Scale bar: 1 mm (B) and 0.5 mm (C).

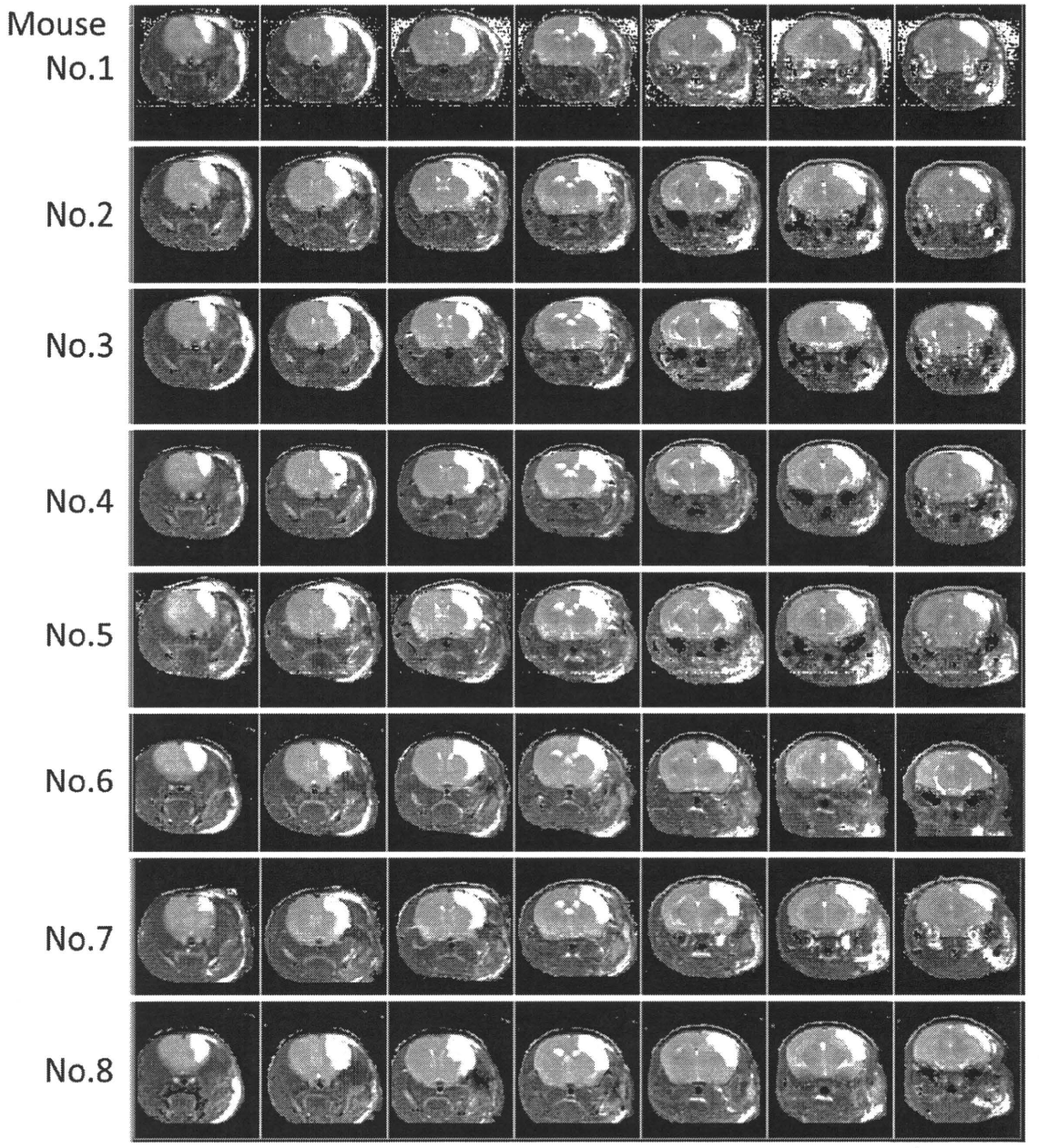

Figure 2. MRI T2 images 24 hours after induction of stroke

The current method results in highly reproducible cortical ischemic damage in all mice.

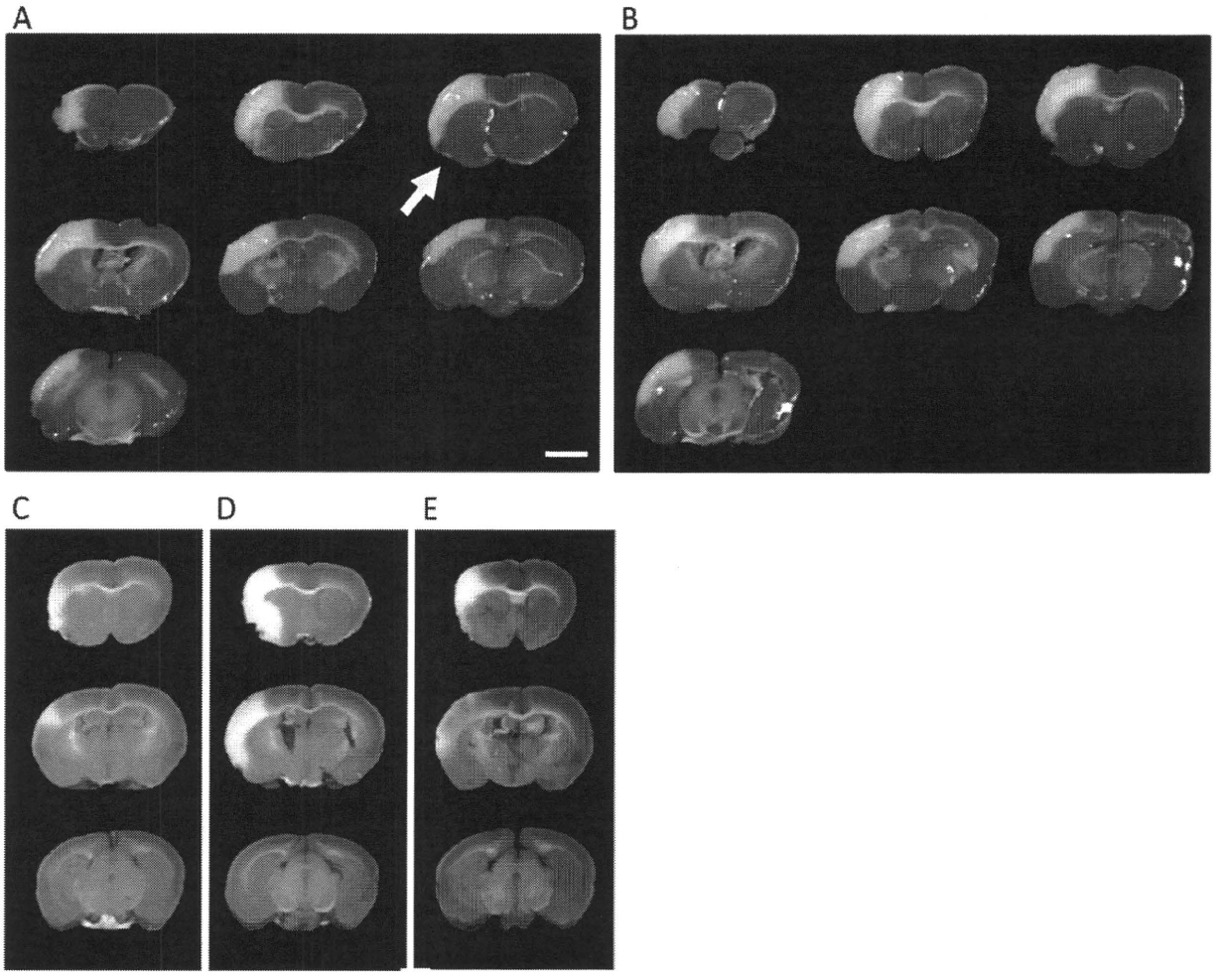

Figure 3. TTC images obtained 24 after stroke

(A,B) Representative images of TTC-stained tissue 24 hours after induction of stroke in CB-17 mice. Similar to the MRI images of SCID mice (Figure 2), reproducible cortical ischemia was observed by TTC staining, comparing the results in different animals. (C–E) Representative images of TTC staining obtained from different C57BL/6 mice are shown. In contrast to the reproducibility of SCID and CB-17 mice, lesion size and even location varied substantially in C57BL/6 mice comparing different animals. Scale bar: 2 mm (A). The arrow indicates the portion around the area subject to electric coagulation (A).

EJN fens EUROPEAN JOURNAL OF NEUROSCIENCE

European Journal of Neuroscience, Vol. 31, pp. 90–98, 2010 doi:10.1111/j.1460-9568.2009.07043.x

NEUROSYSTEMS

Injury-induced neural stem/progenitor cells in post-stroke human cerebral cortex

Daisuke Nakayama,[1,2] Tomohiro Matsuyama,[3] Hatsue Ishibashi-Ueda,[4] Takayuki Nakagomi,[3] Yukiko Kasahara,[1] Haruka Hirose,[1] Akie Kikuchi-Taura,[1] David M. Stern,[5] Hidezo Mori[6] and Akihiko Taguchi[1]

[1]Department of Cerebrovascular Disease, National Cardiovascular Center, 5-7-1 Fujishiro-dai, Suita, Osaka, 565-8565 Japan
[2]Department Cardiac Physiology, National Cardiovascular Center, 5-7-1 Fujishiro-dai, Suita, Osaka, 565-8565 Japan
[3]Institute for Advanced Medical Sciences, Hyogo College of Medicine, Hyogo, Japan
[4]Department of Pathology, National Cardiovascular Center, 5-7-1 Fujishiro-dai, Suita, Osaka, 565-8565 Japan
[5]VPHA and Dean's Office, College of Medicine, University of Cincinnati, OH, USA
[6]Department of Physiology, School of Medicine, Tokai University, Kanagawa, Japan

Keywords: cerebral infarction, cortex, neurogenesis

Abstract

Increasing evidence points to accelerated neurogenesis after stroke, and support of such endogenous neurogenesis has been shown to improve stroke outcome in experimental animal models. The present study analyses post-stroke cerebral cortex after cardiogenic embolism in autoptic human brain. Induction of nestin- and musashi-1-positive cells, potential neural stem/progenitor cells, was observed at the site of ischemic lesions from day 1 after stroke. These two cell populations were present at distinct locations and displayed different temporal profiles of marker expression. However, no surviving differentiated mature neural cells were observed by 90 days after stroke in the previously ischemic region. Consistent with recent reports of neurogenesis in the cerebral cortex after induction of stroke in rodent models, the present current data indicate the presence of a regional regenerative response in human cerebral cortex. Furthermore, observations underline the potential importance of supporting survival and differentiation of endogenous neural stem/progenitor cells in post-stroke human brain.

Introduction

Ischemic events in the central nervous system (CNS), such as stroke, cause permanent neuronal loss and are an important cause of morbidity and mortality in developed countries. Although functional recovery after stroke is limited, multiple studies have demonstrated that the CNS has reparative potential, as exemplified by activation of endogenous neurogenesis following cerebral ischemia (Arvidsson *et al.*, 2002; Taguchi *et al.*, 2004). The subventricular zone (SVZ) of the lateral ventricle and the subgranular zone (SGZ) of the hippocampal dentate gyrus are major regions exhibiting constitutive neurogenesis under physiologic (Kuhn *et al.*, 1996; Alvarez-Buylla & Garcia-Verdugo, 2002) and pathologic conditions (Jin *et al.*, 2001). Recent studies have demonstrated that potential neural stem/progenitor cells are located in a variety of brain regions (Itoh *et al.*, 2005; Kallur *et al.*, 2006; Jiao & Chen, 2008) in addition to the SVZ and SGZ, including the cerebral cortex in post-stroke murine brain (Nakagomi *et al.*, 2009b). Although the contribution of these stem/progenitor cells to CNS repair is still unclear (Magavi *et al.*, 2000; Jiao & Chen, 2008; Nakagomi *et al.*, 2009b), neural stem/progenitor cells obtained from post-stroke cortex have been shown to form neurosphere-like cell clusters and differentiate *in vitro* into mature neurons with characteristic electrophysiologic properties (Nakagomi *et al.*, 2009b). Moreover, recent reports have demonstrated potential neural stem/progenitor cells in human brain, although the origin of these cells has not been determined (Schwartz *et al.*, 2003; Jin *et al.*, 2006; Richardson *et al.*, 2006).

In the current study, we investigated the temporal and spatial expression of nestin and musashi-1, markers associated with neural stem/progenitor cells, in autoptic human brain from patients who suffered cardiogenic cerebral embolism. We have found induction of potential neural stem/progenitor cells, based on expression of these markers, in post-stroke human cortex. These findings, we believe, provide the basis for a potential therapeutic strategy buttressing survival and differentiation of endogenous neural stem/progenitor cells in patients after stroke.

Materials and methods

Patients

Cases of cardiogenic cerebral embolism which were serially autopsied between 2001 and 2004 at the National Cardiovascular Center were entered into this study. The diagnosis of cardiogenic cerebral embolism was made by neurologists according to clinical guidelines

Correspondence: Dr Akihiko Taguchi, as above.
E-mail: taguchi@ri.ncvc.go.jp

Received 6 July 2009, revised 2 November 2009, accepted 2 November 2009

TABLE 1. Baseline characteristics

Patient no.	Days after stroke	Age (years)	Sex	Risk factor				Territory of infarction
				HT	DM	HL	SM	
1	1	71	M	+	+	−	−	Bil. PCA, BA
2	4	34	F	+	−	−	−	R.ACA, R.MCA, BA
3	8	63	M	−	−	+	−	L.MCA
4	8	84	M	+	+	+	+	Bil.ACA, L.MCA, R.PCA
5	10	81	M	+	−	−	+	Bil.ACA, Bil.MCA
6	17	71	F	+	+	−	−	R.MCA, R.ACA
7	24	80	M	+	+	+	+	L.PCA
8	30	71	F	+	+	+	−	R.MCA
9	90	65	M	+	+	+	+	R.MCA
10	360	71	F	+	+	+	−	L.MCA

HT, hypertension; DM, diabetes mellitus; HL, hyperlipidemia; SM, smoking. Bil., bilateral; R, right; L, left. ACA, anterior cerebral artery; MCA, middle cerebral artery; PCA, posterior cerebral artery; BA, basilar artery.

(Cerebral Embolism Task Force, 1986) and the stroke-affected region was evaluated by computed tomography (CT) or magnetic resonance imaging (MRI). All brain samples were obtained with informed consent of autopsy from families (n = 10). Baseline characteristics of the patient population are shown in Table 1. As a control, sections of intact cerebral cortex with no abnormal signal in diffusion-weighted images by MRI (patient number 1) and CT (patient numbers 2–10) from the same stroke patients were obtained.

Preparation of sections and immnohistochemistry

Because of known infiltration and activation of inflammatory cells in post-stroke brain (Kalimo *et al.*, 2002), several cell markers were used to evaluate cells present at the ischemic border.

Brain tissue corresponding to the high-intensity region in diffusion-weighted images from MRI was obtained from patient number 1 (Fig. 1A), fixed in 10% buffered formalin and embedded in paraffin. Tissue sections were evaluated after H&E staining, and the area of cerebral ischemia was determined by the presence of pyknotic morphologic changes and/or loss of nuclei in neurons (Fig. 1B and C). Brain tissue corresponding to low-intensity regions by CT was obtained from patient numbers 2–7 (Fig. 1D). The presence of infiltrating macrophages was evaluated immunohistochemically with anti-CD68 antibody (DAKO, Glostrup, Denmark) (Fig. 1E and F). Similarly, brain tissue corresponding to low-intensity regions by CT was obtained from patient numbers 8–10 (Fig. 1G). Accumulation of astrocytes in the post-stroke area was confirmed using anti-glial fibrillary acidic protein antibody (GFAP; DAKO) (Fig. 1H and I). Serial sections were also examined immunohistochemically using anti-nestin (Millipore, Billerica, MA, USA), anti-musashi-1 (Millipore), anti-βIII-tubulin (Millipore) and anti-CD31 (DAKO) antibodies, as markers of neurogenesis (nestin and musashi-1), neuronal cells (βIII-tubulin) and endothelial cells (CD31), respectively.

All brain sections were processed by microwave treatment for 10 min at 95°C in citrate buffer, pH 6.0. Non-specific binding sites were blocked with a solution containing 0.25% casein, stabilizing protein and 0.015 mol/L sodium azide in PBS (blocking solution; DAKO) for 10 min at room temperature. Then, sections were incubated for 24 h at 4°C with primary antibody in blocking solution. Following incubation of tissue with primary antibody, sections were further incubated for 1 h at room temperature with secondary antibody (DAKO). Antibody binding was visualized by the horseradish-labeled polymer-immunocomplex method using Envison system (DAKO). The chromogen was diaminobenzidine (DAB, dilution 1 : 500) and the counterstain was hematoxylin. Information concerning the antibodies employed in our study are shown in Table 2. For control experiments, mouse-monoclonal and rabbit-polyclonal anti-human cardiac Troponin T antibody (ANA spec, Fremont, CA, USA, cat. no. 53924, dilution 1 : 50 and Novus Biologicals, Inc., Littleton, CO, USA, cat. no. NBP1-18285, dilution 1 : 500, respectively) were used. No positive signal was detected with these antibodies in the serial brain sections (data not shown).

Quantitative analysis of nestin- and musashi-1-positive cells in post-stroke cortex

For quantitative analysis, an experienced pathologist blinded to the experimental protocol evaluated the number of nestin- and musashi-1-positive cells in the infarct border area (the latter defined as approximately 1–2 mm from the infarct border) in high-power fields (×100 magnification, 1 mm^2 each, n = 5), based on the morphology of the cells and density of the signal. The number of nuclei with nestin-positive cytoplasma or musashi-1-positive cytoplasma/nuclei was counted as nestin- or musahi-1-positive neural stem cells, respectively. Cells with insufficient signal or aberrant morphology were not counted as positive cells.

Similarly, sections from intact cerebral cortex were evaluated. The absence of pathological changes was confirmed by H&E staining, and serial sections were analysed at each time point with anti-nestin and anti-musashi antibodies (in high-power fields; ×100 magnification, 1 mm^2 each, n = 5). All immunohistochemical analyses were performed using an Olympus AX 80 microscope (Olympus, Tokyo, Japan) with 4 × /(NA 0.10), 10 × /(NA 0.25), 20 × /(NA 0.75) or 40 × /(NA 0.65) objective lens and digital images were acquired using an Olympus DP70 digital camera system (Olympus).

Statistical analysis

The arithmetic mean and standard error were calculated using JMP 7.01 (SAS Institute Inc., Cary, NC, USA). Statistical tests were not performed as a part of this study.

Results

Nestin-positive cells in post-stroke human cerebral cortex

To investigate ischemia-mediated induction of neural stem/progenitor cells in post-stroke cerebral cortex, brain tissue from day 4 after stroke

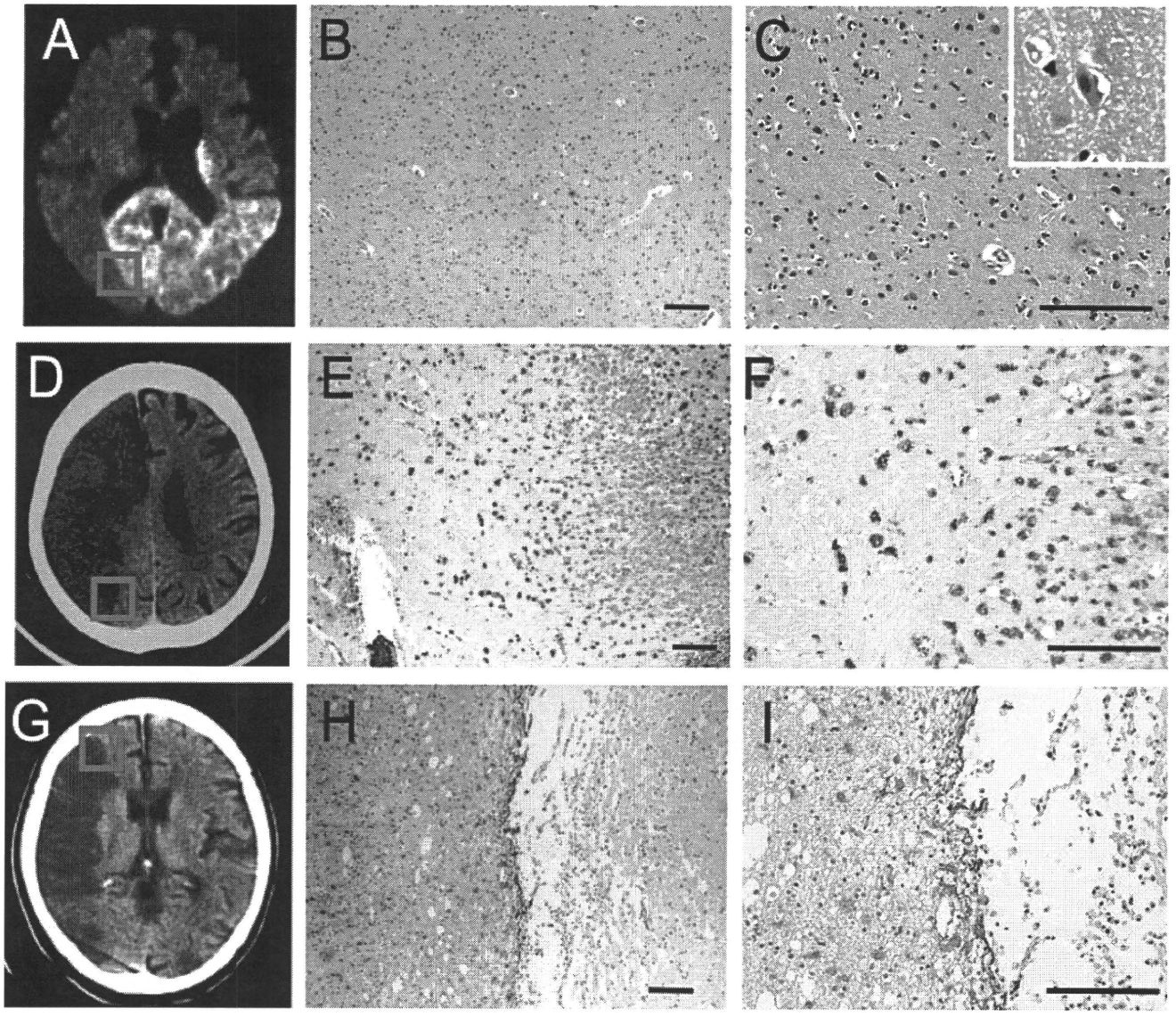

FIG. 1. Representative MRI and CT images from cases of cardiogenic embolism and photomicrographs of the infarcted area after stroke (A, patient No. 1; D, patient No. 6; G, patient No. 9). Box marks in panels A, D and G indicate areas further studied in the peri-infarct zone. Panels B and C show pyknotic changes in nuclei of neurons on day 1 post-stroke visualized with H&E staining (B, lower magnification; C, higher magnification; inset, highest magnification). Panels E and F show numerous infiltrating macrophages (CD68) at 17 days post-stroke (E, lower magnification; F, higher magnification). Panels H and I display reactive astrocytes (GFAP staining) at 90 days after the infarct (H, lower magnification; I, higher magnification). Scale bar: 200 μm.

TABLE 2. Primary antibodies used in this study

Antigen	Host	Source	Cat. no.	Dilution	Antigen
CD68	Mouse	DAKO, Glostrup, Denmark	M0876	1 : 50	Human mononuclear spleen cell preparation containing more than 80% Gaucher's cells
GFAP	Rabbit	DAKO, Glostrup, Denmark	Z0334	1 : 50	Protein isolated from cow
Nestin	Mouse	Millipore, Billerica, MA, USA	MAB5326	1 : 500	Fusion protein
Musashi-1	Rabbit	Millipore, Billerica, MA, USA	AB5977	1 : 500	Synthtic peptide corresponding to residues on the *N*-terminus of human Musashi-1
βIII-tubulin	Mouse	Millipore, Billerica, MA, USA	MAB1637	1 : 500	Synthetic peptide corresponding to amino acids 443–450 of human βIII-tubulin
CD31	Mouse	DAKO, Glostrup, Denmark	M0823	1 : 50	Cell membrane preparation from the spleen of a patient with hairy cell leukemia

was evaluated following staining with H&E (Fig. 2A), or immunohistochemistry with antibodies to CD68 (Fig. 2B) or nestin (Fig. 2C–E; C). Similar to our previous observations in a rodent stroke model (Nakagomi *et al.*, 2009b), induction of nestin-positive cells was observed in post-stroke cortex. Nestin-positive cells were especially evident in proximity to microvasculature. Expression of musashi-1 was

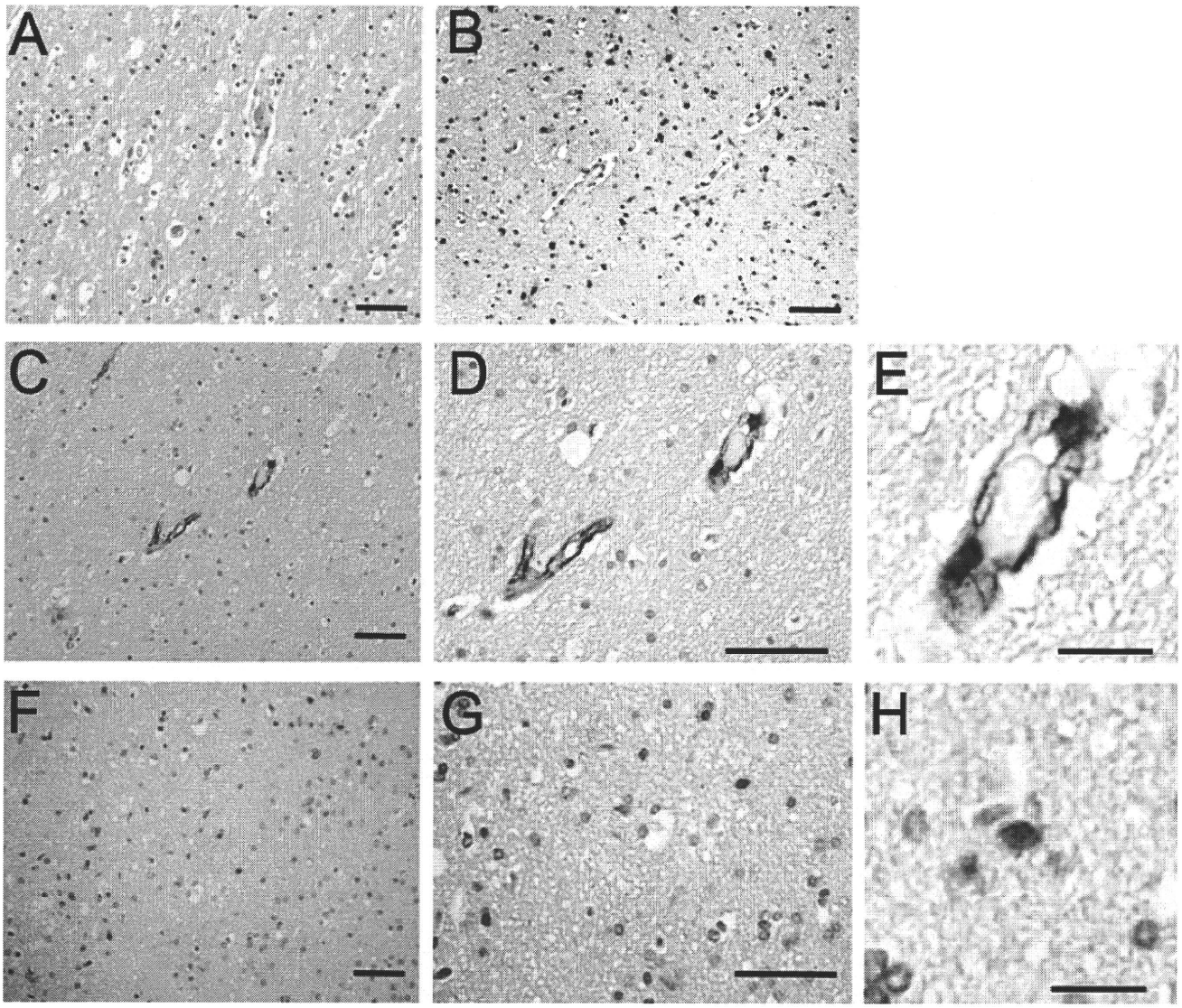

FIG. 2. Nestin-positive cells in post-stroke cortex on day 4 after infarction (A–H, serial sections from patient No. 2). Panel A shows H&E staining and B displays CD68-positive cells. Panels C–H present immunohistochemical detection of nestin (C, lower magnification; D, higher magnification; E, highest magnification) and musashi-1 (F, lower magnification; G, higher magnification; H, highest magnification). Note, most of the nestin-positive cells were located in proximity to vascular-like structures (C–E). Scale bar: 50 μm (A–D, F and G) and 20 μm (E, H).

also investigated; only a few round cells showed weak expression of musashi-1 (Fig. 2F–H). These findings support the presence of ischemia-induced neural stem/progenitor cells in post-stroke human cerebral cortex.

Musashi-1-positive cells in post-stroke human cerebral cortex

On day 4 after stroke, weak (but distinct) expression of musashi-1 was observed in a small population of cells whose morphology and location was different from that of nestin-positive cells. These findings are consistent with previous reports of the presence of a variety of neural stem/progenitor cells in rodent cortex (Belachew *et al.*, 2003; Yokoyama *et al.*, 2006; Nakagomi *et al.*, 2009b). To further investigate injury-induced neural stem/progenitor cells in post-stroke cortex, brain samples on day 10 after stroke were studied (Fig. 3A–C). In contrast to day 4 post-stroke brain, serial sections on day 10 after stroke showed the presence of a significant number of musashi-1-positive cells in the post-stroke area (Fig. 3D–F), although musashi-1 did not co-localize with vasculature. Immunohistochemical analysis with anti-nestin antibody revealed only weak expression in a small number of cells (Fig. 3G–I).

The location of musashi-1-positive cells suggested that this putative neural stem/progenitor cell population was present at a locus distal from the infarct border (i.e. right half of the section). To investigate the nature of this distribution of musashi-1-positive cells, their spatial relationship to the glial response to cerebral infarction was evaluated. Astrocyte activation (GFAP expression) was observed proximal to the infarct border (i.e. left half of the section), although a few activated astrocytes were seen in the distal area as well (Fig. 3C). These findings are consistent with a previous report that neural stem cells are relatively resistant to hypoxia/ischemia after stroke (Romanko *et al.*, 2004), and indicate that induction of musashi-1-positive potential neural stem/progenitor cells occurs in the setting of relatively severe ischemia.

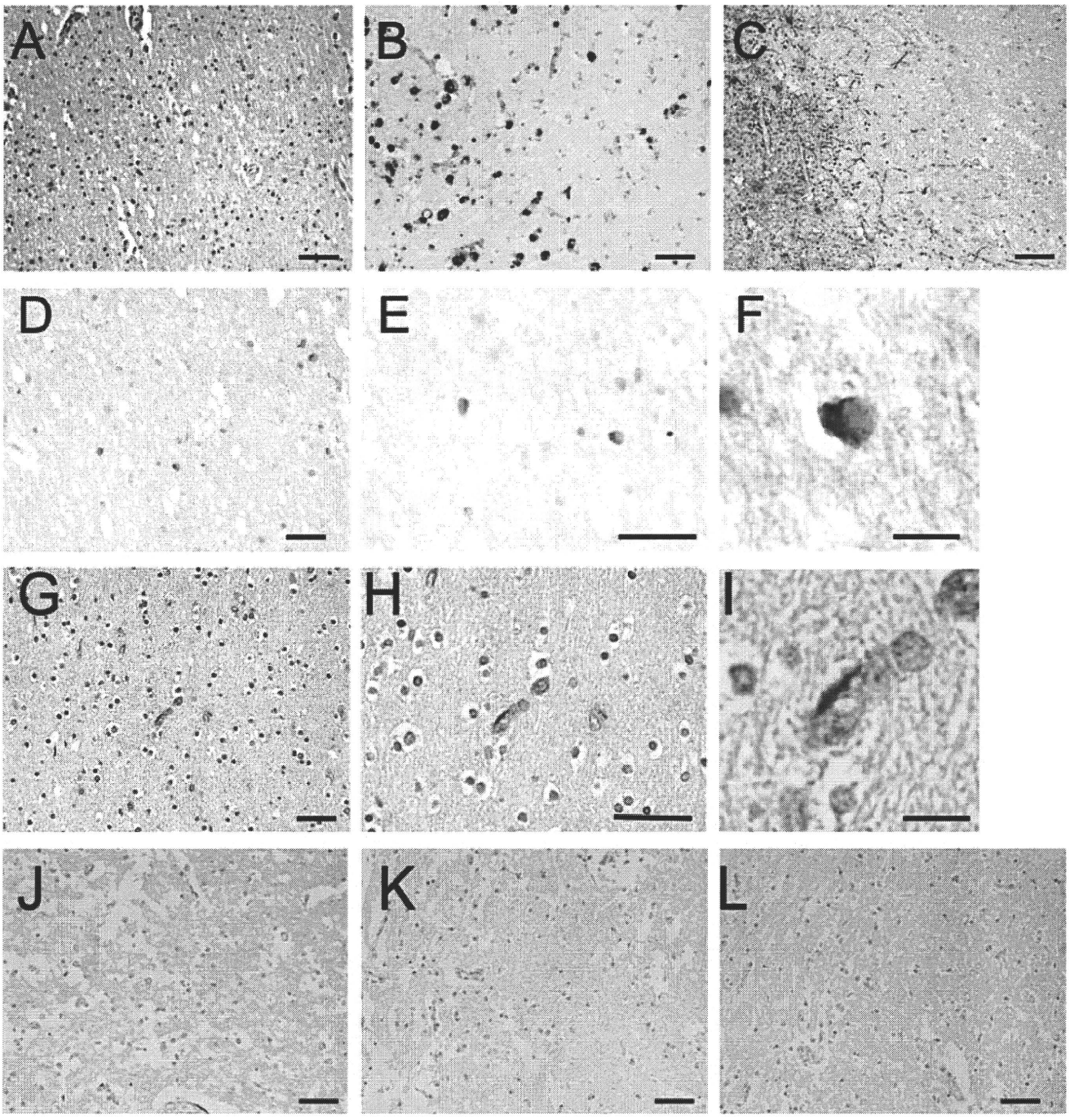

FIG. 3. Mushasi-1-positive cells in post-stroke cortex on day 10 post-infarction. Panels A–I are serial sections from patient No. 5. Panel A shows H&E histology, B shows CD68-positive cells, C displays GFAP-positive cells, and D–I present immunohistochemical detection of musashi-1 (D, lower magnification; E, higher magnification; F, highest magnification) and nestin (G, lower magnification; H, higher magnification; I, highest magnification). In contrast to the section obtained from tissue at 4 days after stroke (Fig. 2, above), multiple round, musahi-1-positive cells were observed. The location of these cells bore no relation to vascular-like structures. Activation of astrocytes was observed in the post-stroke area, mainly in the region proximal to the infarct border. Panels J–L present immunohistochemistry for βIII-tubulin (J), GFAP (K) and CD31 (L) in tissue harvested 90 days after cerebral infarction. No βIII-tublin-positive neuronal cells (L), GFAP-positive glial cells (M) or CD31-positive endothelial cells (N) were observed in the stroke area on post-stroke day 90. Scale bar: 50 μm (A–E, G, H and J–L) and 10 μm (F, I).

To investigate survival and differentiation of progenitor cells in the infarcted cortex, autoptic brain tissue from 90 days after the ischemic insult was interrogated with anti-βIII-tubulin (Fig. 3J) and anti-GFAP antibodies (Fig. 3K), as markers of neuronal and glial cells, respectively. However, the infarcted area was negative for both βIII-tubulin and GFAP, indicating little contribution of neurogenesis in the immediate post-stroke period to ultimate repair of the cerebral cortex. The latter observation is similar to our previous findings in a rodent model (Nakagomi *et al.*, 2009b). Furthermore, microvasculature in the infarcted cortex from 90 days after stroke was investigated with